

## Estimation of the surface energy balance in the Sahelian zone of Western Africa

Henrik Sogaard

Sogaard, Henrik: Estimation of the surface energy balance in the Sahelian zone of Western Africa. *Geografisk Tidsskrift* 88: 108-115. Copenhagen 1988.

*In studies of desertification in the Sahelian zone of Western Africa an improved knowledge of the water and surface energy balance is recognized to be of major importance. Based on micro-climatological measurements collected during an ongoing field study in the northern part of Burkina Faso, a number of methods for deriving surface energy balance are examined. It is found that for the actual case, with profile measurements restricted to two levels above the surface, exact values of the sensible heat flux can accurately be obtained by applying non-dimensional gradients based on the Monin-Obukhov turbulence theory. Utilization of the results for deriving actual evapotranspiration from standard observations is demonstrated, and the paper finally discusses applicability of the results in satellite remote sensing.*

**Keywords:** *Climatology, Energy balance, Sahel, Desertification, Actual evapotranspiration, Sensible heat flux.*

Henrik Sogaard, associate professor, Institute of Geography, University of Copenhagen, Øster Voldgade 10, DK-1350 Copenhagen K.

As an integrated part of the EEC-sponsored project: "Caractérisation par les techniques de télédétection de la dynamique de la désertification à la périphérie du Sahara", a Danish remote sensing project on desertification was initiated in 1987 aiming at the development of algorithms for deriving agro-climatological parameters and vegetation indicators from satellite data. The intention was that these algorithms should be designed for use in a microcomputer-based image processing system. During a parallel phase of the project this low cost image processing system was developed on a microcomputer with a worldwide distribution net. For a further discussion of the image processing system reference is made to Rasmussen et al. (1987).

As most of the existing algorithms for deriving the surface energy balance from satellite were developed and calibrated in other climatic regions and their transferability to the Sahelian zone was not known beforehand, it was decided to conduct a field experiment in a typical part of the area. This was found in the Oudalan province in the northern part of Burkina Faso, approx. 16° N, 0° W., a region with a yearly rainfall of less than 400 mm. A proper climatological description of the region is found in Cochemé and Franquin (1967).

West of Markoye town an automatic agro-climatological station was established within an area designated to the governmental cattle-breeding station called Markoye Ranch. The location of the mast is indicated on fig. 1, and as seen, the mast is surrounded by single acacia-like trees, while the surface is covered by grass and small bushes.

During the rainy season 1987 comprehensive field studies were conducted on both climate and vegetation. The present paper only considers the climatic aspect of the field survey; further details for the rest of the field program are found in Rasmussen et al. (1987).

### METHODOLOGY FOR ENERGY BALANCE STUDIES

The climatological energy balance can be considered to consist of the following four major terms:

1. The radiation balance,  $R_n$ ,
2. The sensible heat transfer,  $Q_h$ , to and from the atmosphere,
3. The latent heat of evaporation/condensation,  $Q_e$ ,
4. The soil heat flux,  $Q_s$ .

In short, the energy balance equation shows how the available surplus of radiation energy is used at the surface. As all other energy terms, e.g. the consumption by photosynthesis, numerically are of much less importance, the energy balance can be formulated as follows:

$$R_n = Q_h + Q_e + Q_s \quad (1)$$

The three right-hand components ( $Q_h$ ,  $Q_e$ ,  $Q_s$ ) are regarded as positive when energy is directed away from the surface toward either atmosphere or soil.

As the field measurements are conducted in a remote area without power supply, it has been necessary to design an equipment which could automatically measure the basic parameters with a minimum of maintenance. The central unit is an Aanderaa datalogger with interchangeable storing unit with a capacity of 65,000 10-bit words.

On the mast 10 of the 12 sensors mounted on two cross bars placed 2.25 m and 8.5 m above soil surface, while two resistance thermometers are buried respectively 1 and 10 cm below the surface. In each level are measured temperature, wind speed and humidity. The sensor-system is constructed by the Norwegian company Aanderaa. During field campaigns all of the sensors are scanned every 10 min.

Two Aanderaa pyrrometers directed upward and downward, respectively, have been applied for estimating the global radiation and the reflected global radiation. In situ both instruments were calibrated against a standard Kipp and Zonen solarimeter.

The thermal infra-red radiation was derived from surface temperature recordings utilizing the Stefan-Boltzmann equation. During field campaigns the surface bright-

ness temperature was measured by use of a Raytek IR-thermometer, and in the rest of the period it was calculated from soil temperature multiplied by the estimated emissivity of 0.95.

The atmospheric counter radiation has been calculated by the Brunt equation, with locally adjusted coefficients (Rasmussen et al. 1987).

The soil heat flux was in some periods recorded by a heat flux plate and the derived thermal conductivity has been used for flux calculation from the recorded soil temperature gradients.

As recording of the  $R_n$  and  $Q_s$ -terms is relatively straightforward, the two remaining terms, namely  $Q_h$  and  $Q_e$ , call for most attention.

#### Vertical transfer of sensible heat

During daytime the Sahelian environment experiences a vigorous heat load on the surface due to solar radiation. Most of the absorbed energy is distributed to the bottom-near air layers by radiation and eddy diffusion. The heating of the air implies a reduction in density which in turn generates a convective circulation. This heat convection, together with the mechanical induced turbulence due to the wind action, is the mechanism for the upward transfer of sensible heat and the downward transfer of momentum.

In the night-time the temperature profile is inverted, there is no heat convection, and even the mechanical turbulence is suppressed due to the dynamic stability of the atmosphere.

The linking between atmospheric stability and wind structure is demonstrated in fig. 2., which shows the vertical differences in wind speed and temperature on 20 January. This day was found, to be typical for the dry season with light wind, mean 2 m/s and mean temperature around 35°C.

During daytime the vertical temperature difference is fairly constant, corresponding to a temperature gradient,  $dT/dz$ , of only  $-4^\circ\text{C}/100\text{ m}$ , which is close to the superadiabatic temperature gradient. The well developed turbulence implies very small vertical differences in speed within the boundary layer. Opposite throughout the night when there occur temperature inversions up to  $20^\circ\text{C}/100\text{ m}$ , the wind speed can nearly double between the two levels.

Most effectively the influence of the turbulence on heat flux can be analyzed by the eddy correlation technique. This method requires both power and computing facility, which are unavailable in the region, so this method was rejected. Instead it was decided to utilize 2-level profile measurements for the atmospheric fluxes. From the discussion in relation to fig. 2 it was clear, however, that standard algorithms assuming near neutral stability could hardly be used. This will be exemplified by inspection of one of the most applied of these equations, namely, the

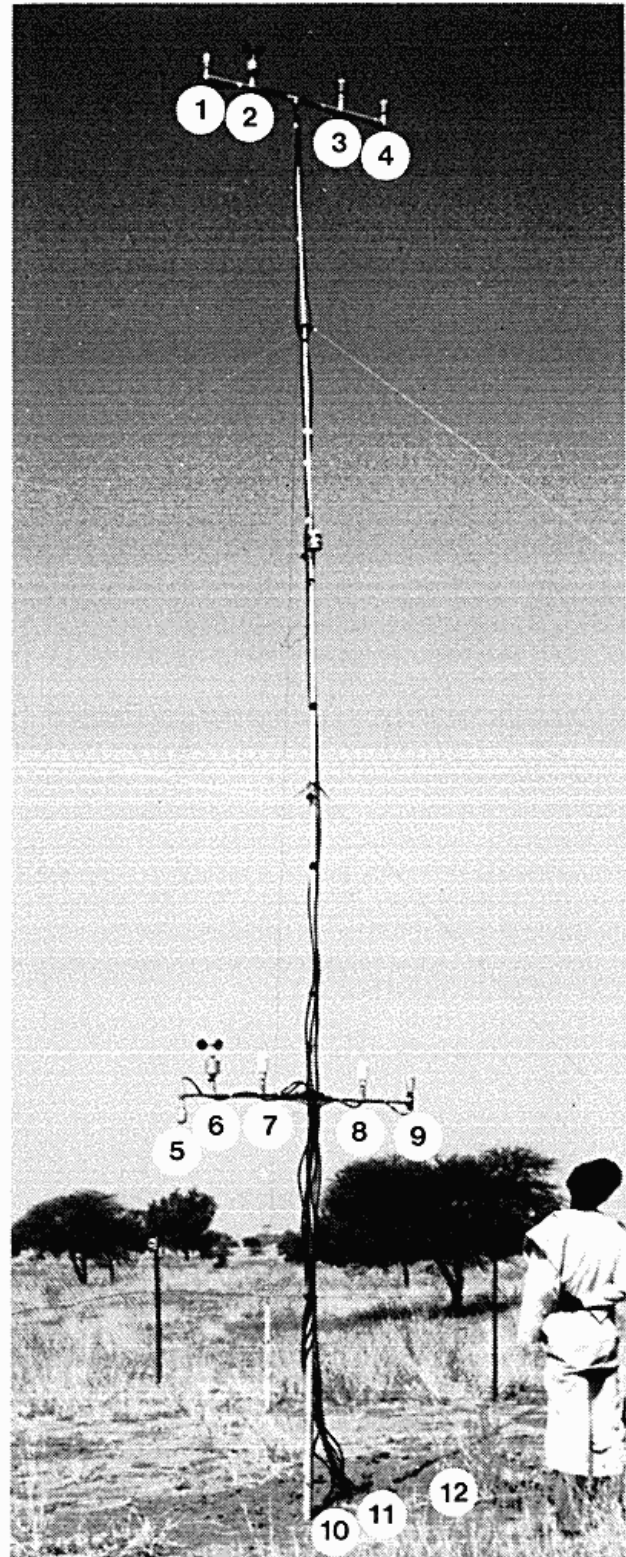


Fig. 1. The climatological profile mast located at Markoye. The numbers refer to the separate sensors discussed in the text.

	Jan	Feb	Mar	Apr	May	Jun	Jul	Aug	Sep	Oct	Nov	Dec	Year
Mean	0	0	1	3	11	57	102	132	61	12	0	0	379
Std.d.	0	1	2	8	12	36	47	46	31	19	1	1	108

Table 1. Monthly mean rainfall and standard deviation, Markoye 1955-86.

Thornthwaite-Holzman formula for deriving sensible heat flux, Deacon (1969). In this formula the flux is obtained by multiplying the gradients in wind speed by gradients in temperature. As demonstrated in fig. 2 this procedure implies systematic errors with overestimation at night and severe underestimation during daytime.

Returning instead to the fundamental expression, the sensible heat transfer can in accordance with molecular diffusion theory be formulated as

$$Q_h = -C_p \rho K_h d \theta / dz \quad (2)$$

where

- $C_p$  is heat capacity for air: 1005 J/kg K
- $\rho$  is air density of the air ( $\approx 1.25 \text{ kg/m}^3$ )
- $K_h$  is the eddy viscosity ( $\text{m}^2/\text{s}$ )
- $d \theta / dz$  is the vertical potential temperature gradient.
- $\theta \approx T + z 0.01$  (dry adiabatic temperature gradient).

Having the dimension square-meter per second,  $K_h$  may be inferred as the product of eddy size and eddy velocity. This implies, however, that  $K_h$  increases non-linearly with the distance from the surface. The  $K_h$  dependency on atmospheric stability, wind speed and elevation makes a substitution of  $K_h$  absolutely necessary for practical use. This will be discussed below.

Similar to equation (2), the flux of momentum, denoted  $\tau$  can be found from

$$\tau = -\rho K_m du/dz \quad (3)$$

#### Characteristics of atmospheric turbulence

For incorporating the atmospheric stability, the gradient Richardson number, defined below, can be applied.

$$Ri = \frac{g d\theta/dz}{T (du/dz)^2} \quad (4)$$

where

- $g$  is the acceleration of gravity
- $T$  is mean temperature, K
- $du/dz$  is the vertical wind speed gradient.

Fig. 3 shows the diurnal variation in  $Ri$  during the two selected days of study, namely the 20 January and the 2 July. In the dry season there are strong oscillations in  $Ri$  during daytime, numbers go from 0 to -10, and a low-pass

filtering of the  $Ri$ -data has been necessary before further processing. Even after filtering distinct fluctuations are observed.

In the beginning rainy season, 2 July, the  $Ri$ -fluctuation is diminished to a level that makes filtering excessive. It is characteristic that with nearly the same radiation heat load the instability is very much less in July than in January. It is further worth noticing that in the dry season there seems to exist an upper  $Ri$ -limit of approximately 0.25. The existence of an upper  $Ri$ -limit, has been discussed by Businger (1971), who points at a number of 0.21, while 0.25 appears in a recent paper by Panopsky and Dutton (1984).

The application of the  $Ri$  in the transfer theory is, however, difficult, as  $Ri$  depends on the distance from the surface. The Monin-Obukhov mixing Length ( $L$ ) defined below, is appropriate alternative, as  $z/L$  is essentially independent of height.

$$L = - \frac{u_*^3 C_p \rho T}{k g Q_h} \quad (5)$$

where

- $k$  is von Karman constant = 0.4.
- $u_*$  is friction velocity.

In the present case with its restricted number of vertical observations, it is impossible, however, to determine the mixing length directly. Instead, the  $Ri$ - $z/L$ -relation formulated by Businger and Dyer (1974) has been applied:

$$\text{atmospheric stability: } \frac{z}{L} = \frac{Ri}{1-5 Ri} \quad (6)$$

$$\text{atmospheric instability: } \frac{z}{L} = Ri \quad (7)$$

#### Implementation of the turbulence theory

It is well-known that under neutral stability, i.e. strong wind and cloudy conditions, the mechanical turbulence will dominate, and here the wind shear ( $du/dz$ ) can be found as

$$\frac{du}{dz} = \frac{u_*}{k z} \quad (8)$$

which by integrating leads to the logarithmic wind profile.

Based on the Monin-Obukhov theory the influence of thermal structure on the wind shear can be formulated by

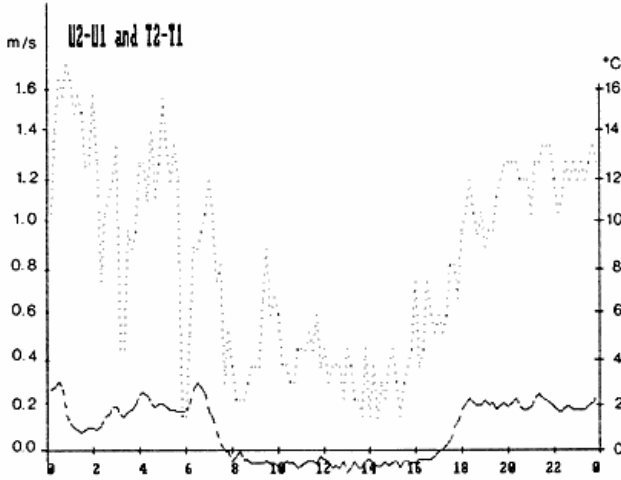


Fig. 2. Diurnal variation in wind speed ( $u_2 - u_1$ ) and air temperature ( $T - T_1$ ) differences between the two levels, 8.5 and 2 m, respectively. The data are from the 20 January 1987.

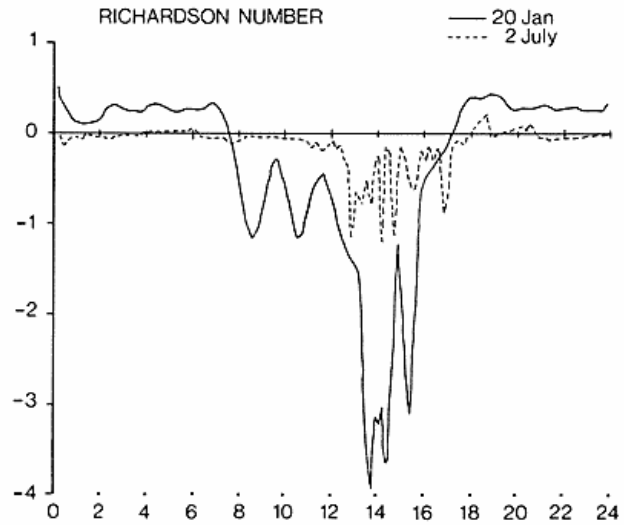


Fig. 3. Diurnal variation in Richardson Number on 20 January and 2 July 1987. The January-data have been filtered through a low-pass filter.

incorporating a non-dimensional function of  $z/L$ , denoted  $\phi_m$

$$\frac{du}{dz} = \frac{\phi_m u^*}{k z} \quad (9)$$

combining the equations (3) and (9), and applying the definition  $u^{*2} = \tau/\rho$ , one obtains

$$K_m = \frac{k z u^*}{\phi_m} \quad (10)$$

dividing by equation (2) gives

$$\frac{C_p \rho u^* k z}{-Q_h} \frac{d\theta}{dz} = \frac{K_m}{K_h} \phi_m \quad (11)$$

comparison with the following equation defining the non-dimensional temperature gradient in accordance with equation (9):

$$\frac{k z}{T^*} \frac{d\theta}{dz} = \phi_h \quad (12)$$

Simple comparison between (11) and (12) shows

$$\phi_h = \frac{K_m}{K_h} \phi_m \quad (13)$$

and, more important,  $-C_p \rho u^*/Q_h$  having the dimension temperature, are assigned the scaling temperature,  $T^*$ ; consequently  $Q_h$  can now be estimated from:

$$Q_h = -C_p \rho u^* T^* \quad (14)$$

## ESTIMATING SCALING TEMPERATURE AND FRICTION VELOCITY

Under unstable conditions

The relation between  $z/L$  and  $\phi_m$  has been formulated in a number of empirical studies during the last twenty years. The one presented below, which is denoted the Businger-Dyer formula, is by far the most widespread, however. For other expressions reference is made to Panofsky and Dutton (1984).

$$\phi_m = \left(1 - 16 \frac{z}{L}\right)^{-1/4} \quad (15)$$

$$\frac{u_2 - u_1}{u^*} = \frac{1}{k} \left[ \ln \left(\frac{z_2}{z_1}\right) + \psi_m \left(z_1/L\right) - \psi_m \left(z_2/L\right) \right] \quad (16)$$

where

$$\psi_m \left(z/L\right) = \ln \left[ \frac{(1+x^2)}{2} \frac{(1+x)^2}{4} \right] - 2 \arctan x + \frac{\pi}{2} \quad (17)$$

and  $x = (1 - 16 z/L)^{1/4}$

The non-dimensional temperature gradient  $\phi_h$  can, according to Businger and Dyer, be devised as:

$$\phi_h = \left(1 - 16 \frac{z}{L}\right)^{-1/2} \quad (18)$$

As shown by Paulson (1970), the following expression is obtained by integration from level  $z_1$  to level  $z_2$ :

$$\frac{\theta_2 - \theta_1}{T^*} = \frac{1}{k} \left[ \ln \left(\frac{z_2}{z_1}\right) + \psi_h \left(z_1/L\right) - \psi_h \left(z_2/L\right) \right] \quad (19)$$

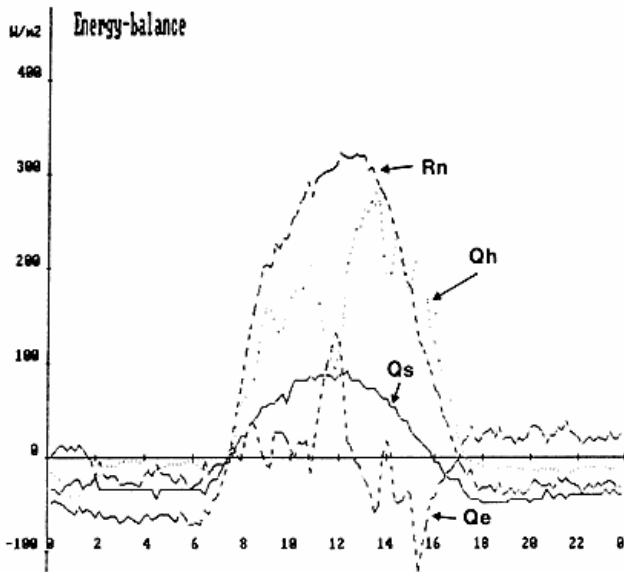


Fig. 4. Diurnal variation in the major energy balance parameters throughout 20 January 1987.

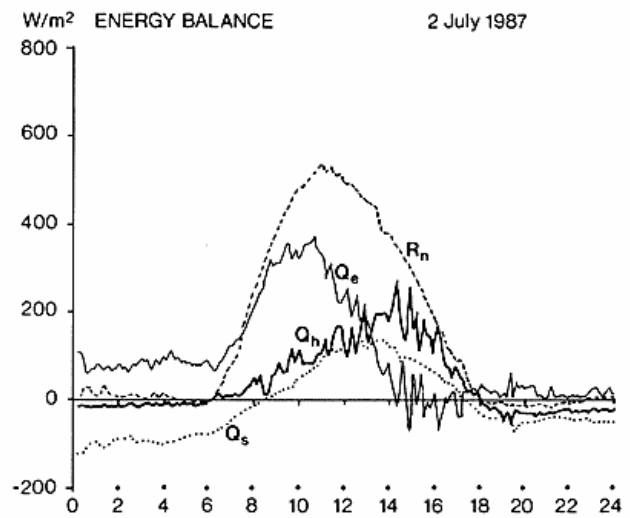


Fig. 5. Diurnal variation in the major energy balance parameters throughout 2 July 1987.

where  $\Phi_h(z/L) = 2 \ln(0.5(1 + \sqrt{1 - 16z/L}))$

Under atmospheric instability,  $Q_h$  can now be derived from equation (14) after solving (16) and (19) for  $T^*$  and  $u^*$  respectively.

#### Sensible heat flux in stable air

In the Businger-Dyer formulation,  $\phi_h$  and  $\phi_m$  are equal under atmospheric stability:

$$\phi_m = \phi_h = 1 + 5z/L \quad (20)$$

By integrating the expression between the two levels the ratio temperature difference divided by scaling temperature is obtained as:

$$\frac{\theta_2 - \theta_1}{T^*} = \frac{1}{k} \left[ \ln \frac{z_2}{z_1} + 5 \frac{z_1}{L} - 5 \frac{z_2}{L} \right] \quad (21)$$

and analogous for the wind:

$$\frac{u_2 - u_1}{u^*} = \frac{1}{k} \left[ \ln \frac{z_2}{z_1} + 5 \frac{z_1}{L} - 5 \frac{z_2}{L} \right] \quad (22)$$

Under stable conditions  $Q_h$  can now be derived from equation (14) after solving (21) and (22) for  $T^*$  and  $u^*$  respectively.

#### DIURNAL VARIATION IN ENERGY BALANCE COMPONENTS

The algorithms given above have been assembled in an interactive Pascal computer program, which runs on the same computer system as used for the image processing mentioned in the introduction. To illustrate the results the variation in each of the parameters is given below for the same two days as shown in fig. 3 (20 January and 2 July) exemplifying the dry and wet season respectively. As 3 of the 4 terms in the balance equation are determined, the last term  $Q_e$  may be found by simple arithmetic.

In fig. 4 is shown the variation in net radiation, sensible heat flux, the soil heat flux and the latent heat flux. Besides  $R_n$ , which is largely mirroring the solar radiation, the sensible heat flux is by far the most important term. In the night the sensible heat flux is directed toward the ground. It is remarkable, however, that due to the laminar flow at night the strong temperature gradient considered in fig. 2 gives only rise to a limited flux of about  $10 \text{ W/m}^2$ .

In fig. 5 is likewise shown the energy balance on 2 July. It is remarkable that the evaporation accounts for most of the energy consumption in the morning, while this term is reduced in the afternoon, when the soil surface becomes dry, and the soil water transfer cannot keep up with the available energy.

#### The energy balance on different days

For intercomparison the procedure has been applied on all data set from the rainy season given in table 2. The individual terms are summarized over a 10 hours period

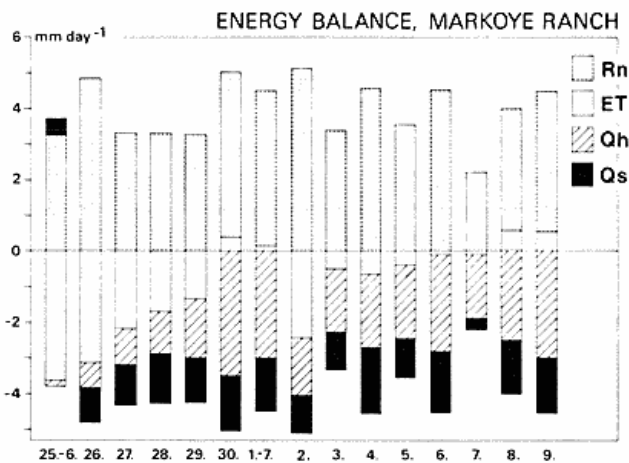


Fig. 6. Variation in daily values in the major energy balance parameters during the first part of the rainy season 1987. Positive values in Qh, ET, Qs are shown downward, negative values upward.

from 7h to 17h. The results have been compared to results derived using the Bowen-ratio approach, and at several occasions it is found that the Bowen-ratio method gives evaporation results which are out of the range between zero and potential evapotranspiration.

Furthermore Bowen-ratio cannot be applied in dry season when there is no measurable water vapor gradient. Consequently it has been decided to estimate Qh from the approach outlined above, while the Qe term is simply found as a residual from the energy equation.

It should be noted that a rather similar procedure has

recently been applied by a French group studying agrometeorology in Senegal (C.N.R.S et al., 1987).

For comparison with evapotranspiration (ET) all the components original calculated in MJ/day have been recalculated to mm of evaporation by dividing with the latent heat of vaporization ( $2.47 \text{ MJ/m}^2$ ); consequently Qe is renamed to ET.

In fig. 6 is shown the variation in the same components during the first part of the rainy season. The effect of the two rainfall events, 24-25 June and 1-2 July, can be easily distinguished. During the next few days the soil surface dries out and Qh increases. It should be noticed that due to cooling effect of the evaporation on 25 June the soil temperature gradient is directed upward supplying the surface with additional energy.

#### Application of the results for Qh

One of the main objectives of the present study has been to elaborate a procedure for estimating actual evapotranspiration from field observations.

The data in table 2 has accordingly been examined in order to know whether Qe or Qh can be obtained from less comprehensive data set, (e.g. standard meteorological observations and/or satellite data).

Day	M	Rn mm/d	ET mm/d	Qs mm/d	Qh mm/d	Sn mm/d	Ts-Ta °C	Ts °C	Rain mm
25	6	3.25	3.65	-0.52	0.12	3.65	1.3	30.6	24.7
26	6	4.82	3.17	0.93	0.73	5.60	6.3	41.3	
27	6	4.31	2.12	1.23	0.97	5.20	8.6	44.0	
28	6	4.28	1.68	1.43	1.17	5.45	11.6	48.2	3.2
29	6	4.27	1.40	1.27	1.60	5.73	15.1	49.3	
30	6	4.76	-0.38	1.57	3.57	6.15	13.4	51.4	
1	7	4.23	-0.17	1.37	3.04	5.51	11.9	49.8	
2	7	5.10	2.44	0.98	1.68	5.67	4.1	42.3	7.5
3	7	3.29	0.46	0.98	1.86	4.22	9.5	41.9	0.3
4	7	4.56	0.67	1.82	2.06	5.74	11.5	50.2	0.1
5	7	3.56	0.38	1.12	2.06	4.50	7.3	41.6	
6	7	4.52	0.11	1.70	2.71	5.78	13.6	51.9	
7	7	2.21	0.10	0.32	1.79	3.18	9.7	37.5	
8	7	3.63	-0.41	1.55	2.49	4.98	14.6	50.7	
9	7	4.04	-0.54	1.57	3.01	5.36	14.7	53.0	

Table 2. The major energy balance components, Markoye Ranch 1987.

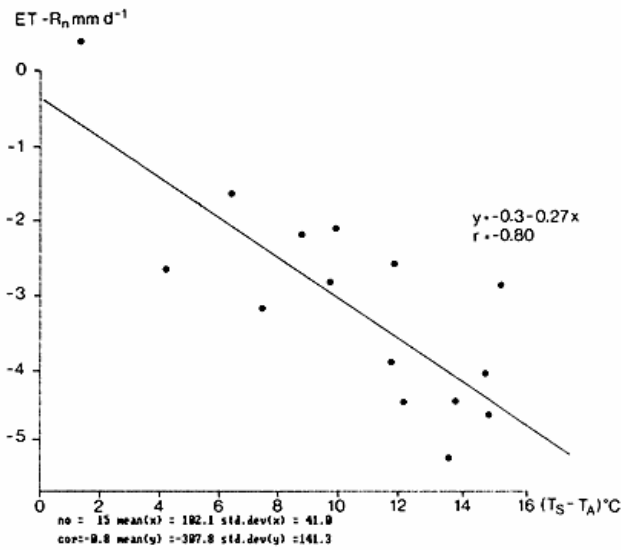


Fig. 7. The difference between evapotranspiration and net radiation as function of midday temperature difference between surface and air. Daily values from Markoye Ranch 25 June - 9 July 1987.

In a study based on data from Sahel, England et al. (1983) have proposed the following simple algorithm for deriving heat flux

$$Q_h = c (T_s - T_a) \quad (23)$$

where

$c$  is a sensible heat transfer coefficient.

$T_s$  is the surface temperature at 14 h local time.

$T_a$  is the air temperature 2 m above surface at 14 h.

Obviously the  $c$ -factor depends on atmospheric stability and wind speed. On basis of the collected wind speed data, which show very little variation in daily mean values, it seems justified to include the wind speed contribution in the "constant".

On the other hand it has been found that the atmospheric stability, and thus heat transfer ability, varies from the dry to the wet season. As the state in the growing season is of major importance, the expression is further examined for only the wet season.

An analysis of the data presented in table 2 shows a significant correlation between  $Q_h$  and  $(T_s - T_a)$  in the first 15 days of the rainy season 1987 ( $r = 0.6$ ).

As the thermal turbulence in the air strongly depends on the heat transport from the soil surface, it is further assumed that the constant  $c$  is mainly a function of the surface temperature, so the air temperature can be ignored in equation (23). This hypothesis is supported by the data in table 2 as the correlation coefficients between

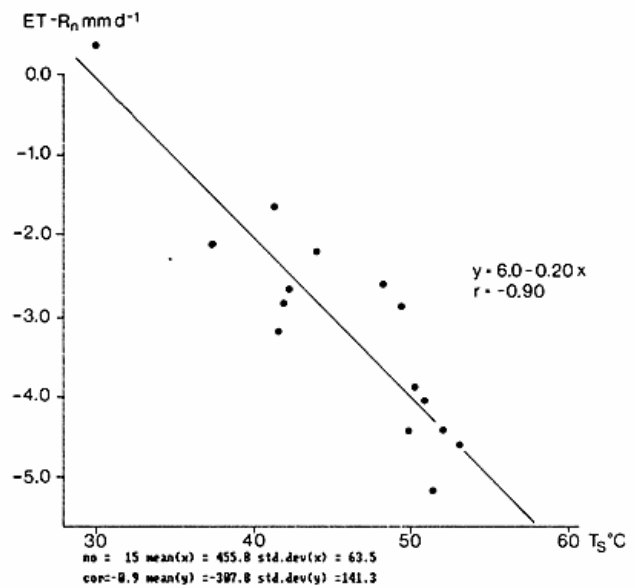


Fig. 8. The difference between evapotranspiration and net radiation as function of midday surface temperature. Daily values from Markoye Ranch 25 June - 9 July 1987.

$Q_h$  and temperature is improved to 0.7 when  $Q_h$  is expressed as a linear function of  $T_s$  only.

Even though some deviations occur, it seems reasonable to assume that for the rainy season in this region the daily sensible heat flux can be estimated from midday soil surface temperatures.

#### Applicability for estimating evapotranspiration

The sensible heat flux is, however, of little practical use compared to the last term of the equation namely actual evapotranspiration. By a further elaboration of equation (1) and (23) it may be assumed that the actual evapotranspiration,  $ET$ , can be found as

$$ET - R_n = a (T_s - T_a) + b \quad (24)$$

where the right-hand term covers combined sensible heat flux and soil heat flux.

Linear regression on the points given in table 2, leads to the following relationship, shown in fig. 7:

$$ET - R_n = -0.3 - 0.27(T_s - T_a) \quad (25)$$

By this approach, adopted from B. Seguin (1983), it is notable that the determined slope coefficient is practically identical with the coefficients given in the quoted studies and later confirmed in the most recent papers (Vidal, 1987).

As it was the case with the sensible heat flux the degree of statistical significance is even improved by utilizing a

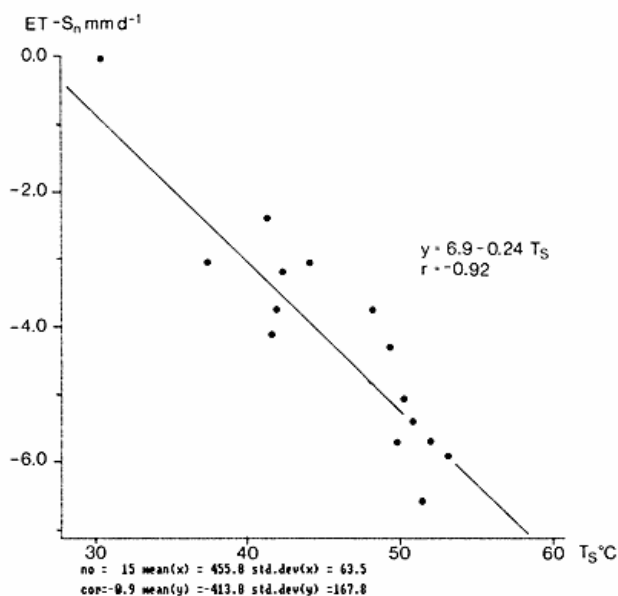


Fig. 9. The difference between evapotranspiration and net global radiation as function of midday surface temperature. Daily values from Markoye Ranch 25 June - 9 July 1987.

linear equation on  $T_s$  only, cfr. fig. 8.

A further inspection of the data reveals that the deficit in daily thermal infrared radiation is highly correlated with surface temperature, and it is thus rational to reduce the equation even further by substituting the absorbed global radiation ( $S_n$ ) for the net radiation. This leads to the following expression:

$$ET - S_n = 6.9 - 0.24 T_s \quad (26)$$

The function is shown in fig. 9, and it is remarkable that the significant correlation is retained (-0.92), and that ET can be derived from standard observations by applying equation (26).

## CONCLUSION

It has been found when applying the Monin-Obukhov theory with a number of adjustments proposed in particular by Businger and Dyer it is possible to derive consistent data on the sensible heat flux from 2-level measurements on wind speed and air temperature in the Sahelian zone of Western Africa.

The collected data support most clearly the linear model approach for deriving evapotranspiration from radiation combined with midday surface- and air temperatures. The slope of this linear function is found to be equal to what is found in studies conducted in regions with subtropical climates.

Further reduction of the model parameters shows that the actual evaporation can be estimated from data di-

rectly available from satellite observations, namely surface temperature and absorbed global radiation.

Due to the agreement with the quoted studies, it seems, justified to conclude that the results support the view that actual evapotranspiration in this part of Sahel can be monitored directly by using satellite data even though the general validation is not, yet, completed.

## ACKNOWLEDGMENTS

The present work has been funded by EEC, DGVIII, to whom the author wishes to express his gratitude. Thanks is due to Anette Reenberg, Søren Kristensen and Carsten E. Hansen for kind assistance during the field work in Burkina Faso.

## References

- Businger, J. A., Wyngaard, J. C., Izumi, Y. & Bradley, E. F. (1971): Flux profile relationships in atmospheric surface layer. *J. Atm. Sci.* Vol. 28, p. 181-189.
- C.N.E.S, I.N.R.A, I.R.A.T., I.S.R.A. & D.M.N. (1987): Suivi du bilan hydrique à l'aide de la télédétection par satellite. Application au Sénégal. Rapport Final.
- Cochemé, J. & Franquin, P. (1967): An agroclimatology survey of semiarid areas in Africa south of the Sahara. WMO Techn. Note 86.
- Deacon, D. L. (1969): Physical Processes Near the Surface of the Earth. In *World Survey of Climatology*, Vol 2, p. 39-103.
- Dyer, A. J. (1974): A review of flux-profile relationships. *Boundary-Layer Meteorol.* Vol. 7, p. 363-372.
- England, C. E., Gombeer, R., Hechinger, E., Herschy, R. W., Rosema, A. & Stroosnijder, L. (1983): The Group Agromet Monitoring Project: Application of Meteosat Data for Rainfall, Evaporation, Soil-Moisture and Plant-Growth Monitoring in Africa. *ESA Journ.* Vol. 7, p. 169-188.
- Panofsky, H. A. & Dutton, J. A. (1984): *Atmospheric Turbulence. Models and Methods for Engineering Applications.* John Wiley & Sons, New York, 1984.
- Rasmussen, K., Folving, S., Holm, J. & Søgaard, H. (1987): Microcomputer oriented methodologies for deriving agro-climatology parameters and vegetation indicators from satellite data. Final Report, internal CEC-report.
- Seguin, B. & Itier, B. (1983): Using Midday Temperature to Estimate Daily Evaporation from Satellite Thermal IR data. *Int. Journ. Rem. Sens.* Vol. 4, p. 371-383.
- Vidal, A., Kerr, Y., Lagouarde, J. P. & Seguin, B. (1987): Télédétection et bilan hydrique: utilisation combinée d'un modèle agrométéorologique et des données de l'IR thermique satellite NOAA-AVHRR. *Agr. Met.* Vol. 39, p. 155-176.



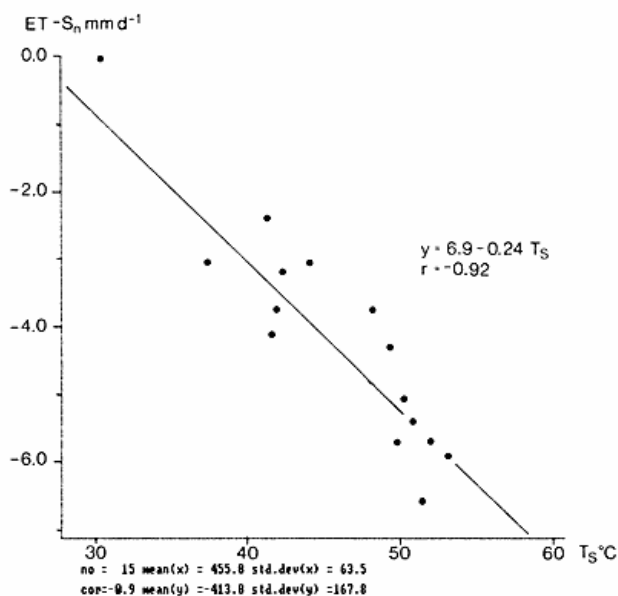


Fig. 9. The difference between evapotranspiration and net global radiation as function of midday surface temperature. Daily values from Markoye Ranch 25 June - 9 July 1987.

linear equation on  $T_s$  only, cfr. fig. 8.

A further inspection of the data reveals that the deficit in daily thermal infrared radiation is highly correlated with surface temperature, and it is thus rational to reduce the equation even further by substituting the absorbed global radiation ( $S_n$ ) for the net radiation. This leads to the following expression:

$$ET - S_n = 6.9 - 0.24 T_s \quad (26)$$

The function is shown in fig. 9, and it is remarkable that the significant correlation is retained (-0.92), and that ET can be derived from standard observations by applying equation (26).

## CONCLUSION

It has been found when applying the Monin-Obukhov theory with a number of adjustments proposed in particular by Businger and Dyer it is possible to derive consistent data on the sensible heat flux from 2-level measurements on wind speed and air temperature in the Sahelian zone of Western Africa.

The collected data support most clearly the linear model approach for deriving evapotranspiration from radiation combined with midday surface- and air temperatures. The slope of this linear function is found to be equal to what is found in studies conducted in regions with subtropical climates.

Further reduction of the model parameters shows that the actual evaporation can be estimated from data di-

rectly available from satellite observations, namely surface temperature and absorbed global radiation.

Due to the agreement with the quoted studies, it seems, justified to conclude that the results support the view that actual evapotranspiration in this part of Sahel can be monitored directly by using satellite data even though the general validation is not, yet, completed.

## ACKNOWLEDGMENTS

The present work has been funded by EEC, DGVIII, to whom the author wishes to express his gratitude. Thanks is due to Anette Reenberg, Søren Kristensen and Carsten E. Hansen for kind assistance during the field work in Burkina Faso.

## References

- Businger, J. A., Wyngaard, J. C., Izumi, Y. & Bradley, E. F. (1971): Flux profile relationships in atmospheric surface layer. *J. Atm. Sci.* Vol. 28, p. 181-189.
- C.N.E.S, I.N.R.A, I.R.A.T., I.S.R.A. & D.M.N. (1987): Suivi du bilan hydrique à l'aide de la télédétection par satellite. Application au Senegal. Rapport Final.
- Cochemé, J. & Franquin, P. (1967): An agroclimatology survey of semiarid areas in Africa south of the Sahara. WMO Techn. Note 86.
- Deacon, D. L. (1969): Physical Processes Near the Surface of the Earth. In *World Survey of Climatology*, Vol 2, p. 39-103.
- Dyer, A. J. (1974): A review of flux-profile relationships. *Boundary-Layer Meteorol.* Vol. 7, p. 363-372.
- England, C. E., Gombeer, R., Hechinger, E., Herschy, R. W., Rosema, A. & Stroosnijder, L. (1983): The Group Agromet Monitoring Project: Application of Meteosat Data for Rainfall, Evaporation, Soil-Moisture and Plant-Growth Monitoring in Africa. *ESA Journ.* Vol. 7, p. 169-188.
- Panofsky, H. A. & Dutton, J. A. (1984): *Atmospheric Turbulence. Models and Methods for Engineering Applications.* John Wiley & Sons, New York, 1984.
- Rasmussen, K., Folving, S., Holm, J. & Søgaard, H. (1987): Microcomputer oriented methodologies for deriving agro-climatological parameters and vegetation indicators from satellite data. Final Report, internal CEC-report.
- Seguin, B. & Itier, B. (1983): Using Midday Temperature to Estimate Daily Evaporation from Satellite Thermal IR data. *Int. Journ. Rem. Sens.* Vol. 4, p. 371-383.
- Vidal, A., Kerr, Y., Lagouarde, J. P. & Seguin, B. (1987): Télédétection et bilan hydrique: utilisation combinée d'un modèle agrométéorologique et des données de l'IR thermique satellite NOAA-AVHRR. *Agr. Met.* Vol. 39, p. 155-176.